Vol. 394: 1–19, 2009
doi: 10.3354/meps08297

MARINE ECOLOGY PROGRESS SERIES
Mar Ecol Prog Ser

Published November 18

OPEN ACCESS

FEATURE ARTICLE

Long-term changes in temperate Australian coastal waters: implications for phytoplankton

P. A. Thompson[1,*], M. E. Baird[2], T. Ingleton[3], M. A. Doblin[4]

[1]CSIRO Division of Marine and Atmospheric Research, GPO Box 1538, Hobart, Tasmania 7001, Australia
[2]School of Mathematics and Statistics, University of New South Wales, Sydney, New South Wales 2052, Australia
[3]Department of Environment and Climate Change, PO Box A290, Sydney South, New South Wales 1232, Australia
[4]Plant Functional Biology and Climate Change Cluster, University of Technology, Sydney, PO Box 123, Broadway, New South Wales 2007, Australia

ABSTRACT: A ~60 yr physical and chemical data set from 4 coastal stations around Australia plus remotely sensed SeaWiFS and phytoplankton taxonomic data were used to evaluate the temporal and spatial variation in phytoplankton ecology. The most consistent trend observed at all stations was a long-term increase in surface salinity of ~0.003 ± 0.0008 psu yr^{-1}. All stations showed positive trends in temperature, with the fastest surface warming (0.0202°C yr^{-1} over 60 yr) in the western Tasman Sea. Long-term trends in warming and stratification were more evident in some months and were not well characterized by annual averages. There was no general pattern of increasing stratification (0 to 50 m); only some stations and a few months showed significant changes. Long-term trends in surface nitrate and phosphate concentrations were either not significant (3 instances) or positive (5 instances) and were up to 6.1 nM phosphate yr^{-1}. A pronounced decline in silicate was evident at the 3 east coast stations, with concentrations falling by as much as 58 nM yr^{-1} over the last ~30 yr. The western Tasman Sea experienced a ~50% decline in the growth rate and biomass of the spring bloom from 1997 to 2007, while other sites showed significant temporal variability in chlorophyll *a* that was associated with the Southern Oscillation Index (SOI). Diatoms tended to dominate the microplankton, especially during periods of low stratification. In conclusion, the physical, chemical and biological properties of Australian temperate waters have changed considerably over the last 60 yr in response to variation in the SOI and the strengthening East Australian Current.

KEY WORDS: Salinity · Temperature · Chlorophyll *a* · Nutrients · Climate change · Stratification

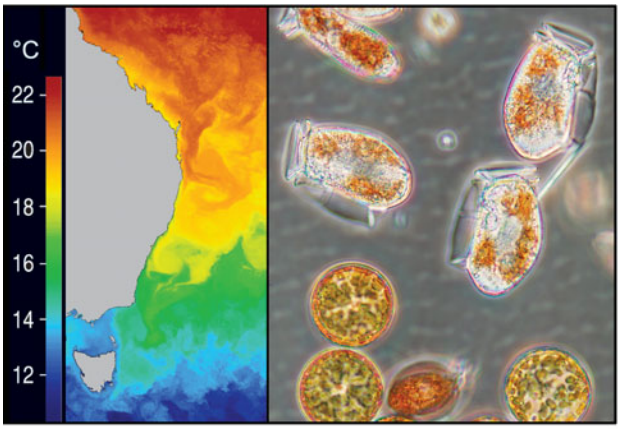

Sea surface temperature (SST) image showing southerly flow of the East Australian Current (left); long-term increase in this flow has led to more dinoflagellates and weaker spring blooms (right) off SE Australia.

Image courtesy of P. Bonham, C. Rathbone, L. Bell (CSIRO)

INTRODUCTION

In their 2007 synthesis, the Intergovernmental Panel on Climate Change (IPCC) used only 30 physical and biological marine data series compared to 527 suitable data series from terrestrial biological systems (Rosenzweig et al. 2007). As a result, the total number of significant biological changes identified in marine and freshwater systems was < 0.3% of their terrestrial counterparts (Rosenzweig et al. 2007). While the high cost of marine research and the IPCC's stringent requirements for data inclusion may explain the terrestrial bias, there is a clear knowledge gap that the marine science community must address (Richardson & Poloczanska 2008). The ocean has been the subject of a number of large,

*Email: peter.a.thompson@csiro.au

cooperative international programs aimed at better understanding processes including biogeochemical cycling and carbon flux (e.g. World Ocean Circulation Experiment [WOCE], Joint Global Ocean Flux Study [JGOFS]); however, there are very few long-term data series that can be used to evaluate the effects of climate variability or climate change. Three of the longest time series, Bermuda Atlantic Time Series (BATS), Hawaii Ocean Time Series (HOTS) and Ocean Station Papa (OSP), are all based in the northern hemisphere and in the deep (>4400 m) ocean. They are therefore representative of only some ocean biogeochemical provinces (Longhurst 1995, 1998) and may not be suitable for assessing climate impacts in the coastal ocean. Despite the general lack of marine baseline data, there are some recent documented changes in phytoplankton dynamics including alterations to species distributions, phenology (annual bloom dynamics) and species composition (Beaugrand 2004, Edwards & Richardson 2004, Hays et al. 2005). Analysis of remotely sensed chlorophyll *a* (chl *a*) data from the global ocean has also shown strong increases in biomass in some regions (Gregg et al. 2005) and modelling suggests biomass could decrease or increase depending upon location (Sarmiento et al. 2004). These variations in biomass could have flow-on effects including increased mismatches in reproductive timing (Cushing 1974) between predators and prey (Richardson & Schoeman 2004, Wiltshire et al. 2008). As phytoplankton are responsible for >40% of global carbon fixation and are the basis of marine food webs (Falkowski & Raven 2007), a decrease in the efficiency of trophic transfer could reduce fisheries production (Chassot et al. 2007) and impact biogeochemical cycling and carbon export to the deep ocean.

The longest records to assess climate impacts on temperate phytoplankton in the southern Pacific and Indian Oceans come from 4 monitoring stations around Australia. Two monitoring stations (Port Hacking 50 m and Maria Island) were established in 1944, a third (Rottnest Island) in 1951 and the fourth (Port Hacking 100 m) in 1953 (Fig. 1). Now in operation for over 55 yr, these data sets are well suited to assessing changes in the physical and chemical properties of continental shelf waters and evaluating their potential impacts on phytoplankton ecology. For example, increased vertical stratification due to surface warming is hypothesized to decrease the upwards flux of nutrients and cause a decline in phytoplankton abundance (Scavia et al. 2002).

In the present study, we investigated temporal patterns of physical and chemical properties and compared them with local phytoplankton floristic data (where available) and satellite-derived estimates of chl *a*. The analyses were undertaken to examine the seasonal dynamics of the regions, to find evidence of long-term surface warming, increased strength or period of vertical stratification possibly resulting in a diminished nutrient availability in the euphotic zone, and to compare these with changes in phytoplankton biomass and composition.

MATERIALS AND METHODS

Oceanographic context. Like elsewhere in the global ocean, primary production in Australian waters is regulated by physical processes that influence light, temperature and the provision of nutrients; processes that have broadly consistent latitudinal patterns (Rudjakov 1997). The Australian continent is unusual, with

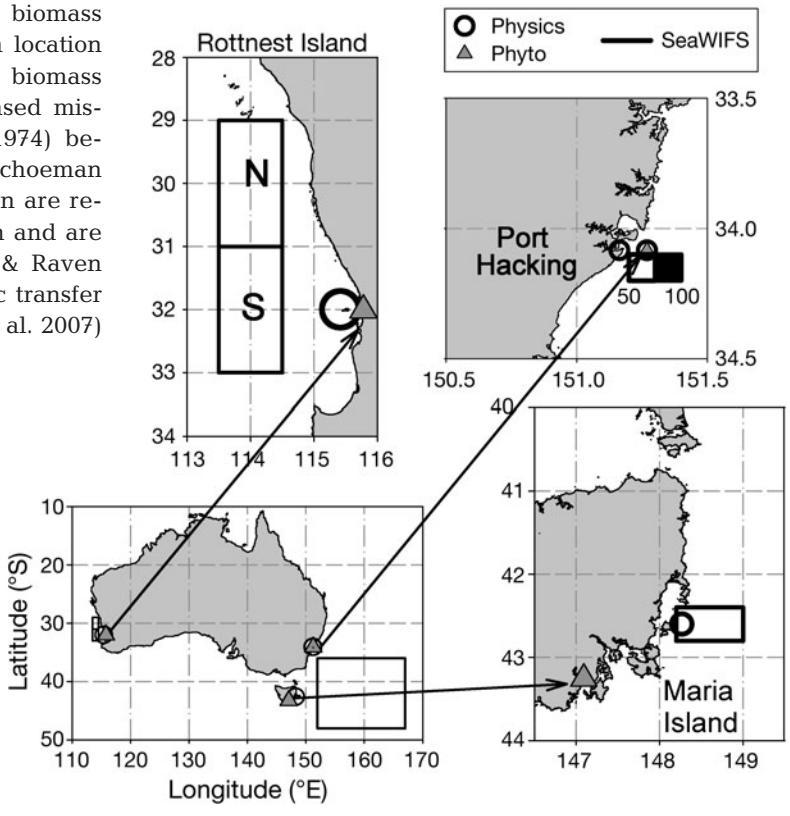

Fig. 1. Location of coastal monitoring stations (○) in temperate Australia where measurements of temperature, salinity and nutrients were made at: ~0, 10, 20, 30, 40 and 50 m, ca. monthly since ca. 1944 (see Tables 1 & 2 for specific details). Also shown are nearby locations where phytoplankton samples for pigments or cell counts (△) were collected (see Table 3 for details) and areas (□) from which remotely sensed ocean colour data were obtained from NASA's Goddard Earth Sciences (GES) Data and Information Services Center (DISC) via the GES-DISC Interactive Online Visualization and Analysis Infrastructure (GIOVANNI) program

poleward flowing currents along both east and west coasts, transporting warm tropical ocean waters southward. The seasonality of the flow is different between coasts, with the west coast Leeuwin Current transporting 2 to 3 Sverdrups (Sv) southward (at 32°S) in summer, rising to 5 Sv in winter (Feng et al. 2003), while on the east coast the East Australian Current (EAC) flow ranges from 7 Sv in winter to 16 Sv (at 28°S) in summer (Ridgway & Godfrey 1997). Most of the EAC abruptly turns east at ~32°S while about a third continues south towards Tasmania and the Maria Island station (Fig. 1; Ridgway & Godfrey 1997).

Significantly, the southerly flow of the Leeuwin Current suppresses upwelling (an unusual feature for an eastern boundary current that results from poleward flow) that would otherwise supply nutrients to the surface and enhance productivity. As a result, phytoplankton biomass and primary production in southwest Australian waters are relatively low compared to the east coast, and show a winter rather than a spring maximum (Jitts 1969, Koslow et al. 2008). Interannual variability in Leeuwin Current flow and sea surface temperature is related to the El Niño–Southern Oscillation (ENSO) phenomenon (Feng et al. 2003). In contrast, waters of similar latitude on the Australian east coast are approximately twice as productive (Jitts 1965) and show a spring phytoplankton bloom with a second bloom in late summer to early autumn (Humphrey 1963, Hallegraeff & Jeffrey 1993, Ajani et al. 2001). Sporadic increases in primary productivity on the southeast coast are the result of EAC activity that uplifts nutrient-rich slope water onto the shelf and close to the surface (Oke & Middleton 2001), sometimes in association with warm-core (Tranter et al. 1986) or cold-core (Gibbs et al. 1997) eddy formation, often resulting in coastal diatom blooms (Hallegraeff & Reid 1986).

Physical and chemical measurements at coastal stations. With some exceptions, the sampling frequency at the 4 coastal stations ranged from ca. weekly to monthly between 1944 and 2005 (Table 1). Generally data gaps are few and relatively short (months) but measurements of phosphate at Port Hacking were not made from 1985 to 2003 and at Rottnest Island no data were collected from 1956 to 1969 (Table 1). Analysis of silicate concentrations commenced in the 1970s. Typically, discrete bottle samples were collected at 0, 10, 20, 30, 40 and 50 m depths (Table 1) and analysed for salinity, dissolved oxygen and dissolved nutrients. Most analytical methods evolved from manual (Major et al. 1972) to automated (Cowley et al. 1999) during the ~60 yr and the precision improved. Temperature was measured using reversing thermometers mounted on the sides of the sampling bottles with a precision better than ±0.02°C. Bottle samples were analysed for salinity with precision better than 0.003 psu, originally by chemical analysis but for most of the data set by conductivity, currently with a Guildline Autosal™ 8400B instrument. Measurement of dissolved oxygen was by Winkler titration with precision better than 6 µM. Analytical techniques for nitrate and/or nitrite (Wood et al. 1967), silicate (Murphy & Riley 1962) and phosphate (Armstrong 1951) were originally manual but adapted for automation and are currently performed using Quick-Chem™ methods on a flow injection LACHAT® instrument. Data for all 4 coastal stations can be downloaded from the CSIRO Marine and Atmospheric Research Data Trawler (www.marine.csiro.au/warehouse/jsp/loginpage.jsp). Profiles of temperature, conductivity and chl *a* by fluorescence were commenced in 1997 using a Sea-Bird SBE25 at the Port Hacking stations by the New South Wales (NSW) Department of Climate Change.

Phytoplankton data. Phytoplankton species data were collected near Maria Island, Rottnest Island (Fig. 1) and at the Port Hacking 100 m station (PH_{100m}) during independent sampling programs, but all with only limited temporal coverage (Table 2). In the case of Rottnest Island, the phytoplankton data are from the mouth of the Swan River Estuary (Blackwall Reach, ~34 km away) which is fully marine during late summer (Thompson

Table 1. Summary of coastal monitoring station locations used to examine long-term changes in physical and chemical ocean properties. Sampling was approximately monthly, although occasionally some higher frequency observations were obtained. Note change in sampling depths for the Port Hacking 100 m station in 1985

Location	Depths sampled (m)	Start (year)	End (year)	Latitude (°S)	Longitude (°E)
Maria Island	0, 10, 20, 30, 40, 50	1944	2005	42.6	148.2
Port Hacking 50 m	0, 10, 20, 30, 40, 50	1944[a]	2004	34.1	151.2
Port Hacking 100 m	0, 10, 20, 30, 40, 50, 75, 100 (to 1985) 0, 10, 25, 50, 75, 100 (to 2005)	1953[a]	2005	34.1	151.3
Rottnest Island	0, 10, 20, 30, 40, 50	1951[b]	2001	32.0	115.4

[a]Gap in PO_4 measurements from 1985 to 2003
[b]Gap in nutrient measurements from 1957 to 1968; measurements recommenced in 1970

1998) and has a phytoplankton community similar to further offshore (Thompson et al. 2007). Two subsets of depth-integrated Swan River Estuary phytoplankton data from 1994 to 2007 were analysed: (1) weekly samples in February, when river runoff is negligible and the water at this station is fully marine; and (2) all weekly samples from January to April (~15 per year). For Maria Island, phytoplankton samples were available from the mouth of the Huon Estuary, approximately 120 km away, from 3 to 15 stations. These stations were sampled weekly or monthly during 1996–1998 and 2004–2005. The dinoflagellate community in the Huon Estuary is similar to that found 150 km offshore (Thompson et al. 2008) and that at Maria Island (P. A. Thompson unpubl. data). All phytoplankton samples were preserved with acid Lugol's solution (Parsons et al. 1984). Near Maria and Rottnest Islands, flexible tubes were used to collect vertically integrated samples. At the Port Hacking 100 m station, a 35 µm mesh plankton net was hauled from 100 m to the surface (Ajani et al. 2001), samples were settled (after Lund et al. 1958) and the first 100 cells observed were identified and counted. A maximum of 30 fields of view or 400 cells (whichever came first) were enumerated in samples from near Maria Island and Rottnest Island. Cells were examined at 100, 200 or 400× magnification and identified at least to family, but where possible, to genus or species. Pigment samples (only near Maria Island) were analysed by HPLC using methods developed by Wright et al. (1991) for extraction and gradient elution.

Remotely sensed chl *a*. The Sea-viewing Wide Field-of-view Sensor (SeaWiFS) operated from September 1997 collecting ocean colour data in the visible and far red region of the spectrum (412, 443, 490, 510, 555, 670, 765 and 865 nm wavelengths). The 10 yr (September 1997 to September 2007) of ocean colour data used in the present study were downloaded using the GES-DISC Interactive Online Visualization and Analysis Infrastructure (GIOVANNI) as part of NASA's Goddard Earth Sciences (GES) Data and Information Services Center (DISC) chl *a* product. GIOVANNI provides SeaWiFS estimates of chl *a* averaged over 8 or 30 d; both were used as a proxy of phytoplankton biomass depending upon the temporal scale under investigation. The areas assessed were immediately seaward of the coastal stations (Fig. 1) and varied in spatial extent from ~1.2×10^2 to ~2.5×10^4 km^2 (Table 2). A relatively large area close to the coastal station was used, constrained by (1) relatively low spatial heterogeneity in mean annual chl *a* with variation less than a factor of 2 across the entire area, (2) no land or shallows (no depths < 20 m) and (3) consistent temporal trends. The continental shelf waters seaward of the coastal stations are low in chl *a* and light attenuation (e.g. extinction coefficient for PAR ≈ 0.05 m^{-1} offshore of Rottnest, Thompson et al. 2007), such that remote sensing

Table 2. Description of the spatial and temporal sampling for phytoplankton at or near coastal monitoring stations (see Table 1) and areas assessed for chlorophyll *a* (chl *a*) biomass using SeaWiFS

Station	Phytoplankton cell counts							SeaWiFS chl *a* (1997–2007)	
	Location (m)	Depths sampled	Analytical methods	Span	Frequency (no. samples)	Latitude (°S)	Longitude (°E)	Latitude (°S)	Longitude (°E)
Near Maria Island	Huon Estuary, 3–15 locations	Integrating tube 0–12 m	30 fields of view or 400 cells sample^{-1} + HPLC pigments	1996–2005	Variable, ca. weekly or monthly (631)	43.3	147.1	42.2–43.0	148.2–149.0
Port Hacking 100 m	At Port Hacking 100 m station	Vertical haul (0.2 m diam., 35 µm mesh net over 100 m)	First 100 cells	1997–2002 (sampling continued but not analysed)	Variable (24)	34.1	151.3	34.1–34.2 (50 m) 34.1–34.2 (100 m)	151.2–151.3 (50 m) 151.3–151.4 (100 m)
Near Rottnest Island	Swan River, Blackwall Reach	Integrating tube 0–6 m	30 fields of view or 400 cells sample^{-1}	1994–2007	Weekly (649)	32.1	115.8	29–31(N) 31–33(S)	113.5–114.5 113.5–114.5

would detect chl *a* to ~20 m. A deep chlorophyll maximum (DCM) is likely in summer (Koslow et al. 2008), although a DCM should not bias the assessment of temporal trends over time spans >1 yr. At Maria Island, the growth rate of the spring bloom was calculated from a linear regression of the natural log of the remotely sensed mean monthly chl *a* concentrations over the period from July to October (4 mo) over the area from 42.2 to 43° S by 148.2 to 149.0° E (Table 2). One growth rate (=1 regression) was estimated for each year from 1997 to 2006.

Data analysis. To remove seasonal effects, at each site the depth-specific monthly mean value was averaged across the entire data set for each parameter (salinity, temperature, density, nitrate, phosphate, silicate, dissolved oxygen and chl *a*) and then subtracted from each value in the relevant month (Makridakis et al. 1998). The residual variation was examined for association with known <10 yr cycles such as ENSO from the Australian Bureau of Meteorology (www.bom.gov.au/silo/) and the Southern Annular Mode from the US National Oceanic & Atmospheric Administration (www.cdc.noaa.gov/data/climateindices/). The long-term trends were calculated as simple linear regressions of seasonally detrended observations of salinity, temperature, density, nitrate and phosphate over the entire duration of the available data set, irrespective of any data gaps (see Tables 1 & 3), making for the most direct comparison between sites. We note that the observed temporal variation was not monotonic and some of the intermediate variation (1 to 50 yr) was ascribed to other causes such as ENSO. To assess whether the long-term rates of change in temperature and salinity were seasonally consistent, linear regressions were carried out for each month separately using depth-averaged values. Rainfall data were obtained from the Australian Bureau of Meteorology (BOM, Stn 66037, Sydney Airport). Stratification ($\Delta\sigma_t$) was calculated from density (after Fofonoff 1985) at the surface (σ_{t0}) minus either density at 50 m (i.e. $\Delta\sigma_{t50} = \sigma_{t0} - \sigma_{t50}$) or 100 m ($PH_{100m}$ station only).

Physical indices for PH_{100m}. A variety of potential mechanisms have been suggested to contribute to upwelling (Roughan & Middleton 2002) and the variability in chl *a* at Port Hacking. In order to further elucidate the mechanisms, 4 indices were calculated in addition to the Southern Oscillation Index (SOI) and examined for correlations with the monthly 1997 to 2007 SeaWiFS-derived chl *a* anomalies. Temperature anomalies were calculated as the difference between the Bluelink reanalysis (BRAN) ocean state (Oke et al. 2008) and the CSIRO Atlas of Regional Seas climatology (version 2006a, Ridgway & Dunn 2003). From September 1997 to December 2006, BRAN 2.1 fields were used, while BRAN 2.2 fields were used from January 2007 onwards. Monthly alongshore wind anomalies were obtained from the US National Center for Atmospheric Research (NCAR) ¼ degree 6 hourly reanalysis (www.cdc.noaa.gov/data/reanalysis/reanalysis.shtml, Kalnay et al. 1996) minus a climatology calculated from the reanalysis over 10 yr. Wind speed anomalies were similarly calculated using both alongshore and cross-shore winds from the NCAR reanalysis. The final index, the fraction of EAC water, Θ_{100}, was used as a measure of the source waters at the Port Hacking station. A value of 1 implies the water at Port Hacking over the last ~10 to 20 d has come from only southward flow alongshore (i.e. 100% EAC waters). A value of 0 implies only Tasman Sea water. For a derivation of Θ_{100}, see Appendix 1. The index Θ_{100} is useful in distinguishing temperature anomalies that result from horizontal water mass movement versus those cooling events that are more localised and non-upwelling. It also provides a measure of the relative strength of the EAC.

RESULTS

Seasonal dynamics by site

In this section of the 'Results' we present analyses of the seasonal dynamics at each site. Generally, these seasonal trends are removed from the analyses presented in 'Detailed location-specific changes'. This section also contains station inter-comparisons for long-term stratification and temperature trends by month as well as winter nitrate concentrations versus temperature.

Temperature

All stations showed similar patterns of seasonal surface water temperature variation, but the annual minima occurred in August for Port Hacking, September for Maria Island and October for Rottnest Island (Fig. 2A). The Port Hacking 50 (PH_{50m}) and PH_{100m} stations had the greatest seasonal amplitude (~5.3°C, Fig. 2A) followed by Maria Island (~5.0°C) and Rottnest Island (~3.2°C).

Salinity

All stations were highly marine (>35 psu) throughout the year, with seasonal amplitudes of <0.5 psu (Fig. 2B). Unlike temperature, the seasonal dynamics of surface salinity were markedly different across sites (Fig. 2B), with salinity increasing during winter on the east coast reaching maxima in July at the PH_{50m} and PH_{100m} stations, and decreasing on the west coast at Rottnest Island to a minimum in July. Maria Island had a seasonal salinity minimum in spring.

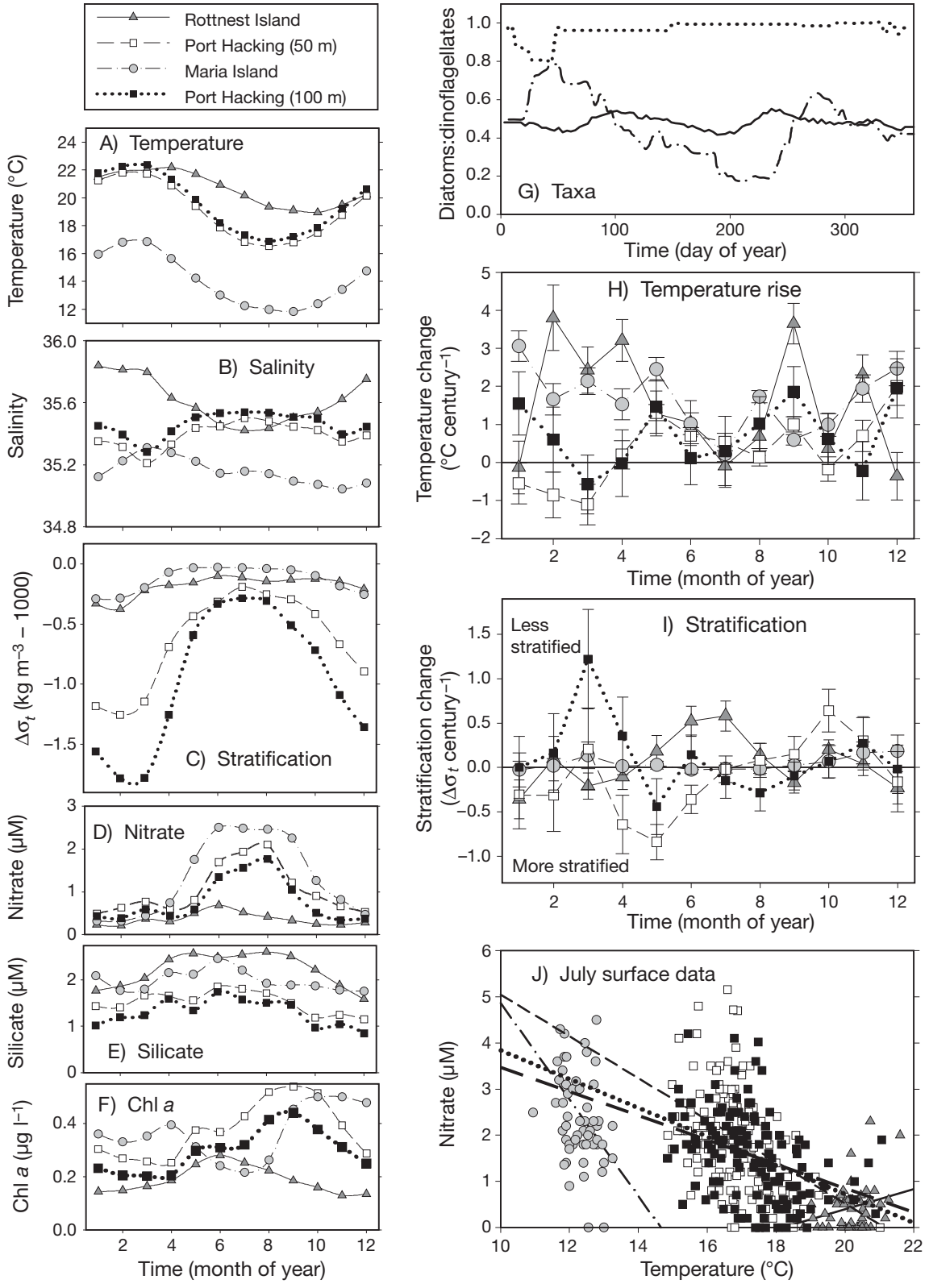

Fig. 2. Monthly mean surface (A) temperature, (B) salinity, (C) vertical stratification, (D) dissolved nitrate and (E) dissolved silicate from coastal monitoring stations around temperate Australia from 1942 to 2007 (see Table 2 for sample details). (F) Satellite-derived mean monthly chlorophyll *a* between 1997 and 2007 from areas near each coastal station (see Fig. 1 for details) and (G) running average ratio of diatoms:dinoflagellates (sample details in Table 2). Long-term trends in monthly (H) surface temperature and (I) vertical stratification at coastal stations (Table 3, Fig. 1) from least squares fit of the monthly temperature anomaly versus time; error bars are SE of the slope. (J) Regressions of surface temperature with surface nitrate at coastal stations (see Table 3). Lines are extended to axis for clarity; heavy long dash is the mean of all data, others as stipulated in key

Nutrients

Low surface nitrate concentrations (<0.5 µM) were typical of all stations during the austral summer (Fig. 2D). All stations showed a slight rise in average surface nitrate in March with concentrations at Rottnest Island and Port Hacking then declining in April before rising steadily to peak in winter. The amplitude of these annual nitrate cycles was significantly different between stations, with peak surface concentrations in mid-winter nearly 10 times greater at Maria Island compared to Rottnest Island. Average surface phosphate concentrations had similar seasonal dynamics to those for nitrate, such that the average monthly surface values (12 per station) were highly correlated with average monthly surface nitrate across all 4 stations ($r^2 = 0.74$, $p < 0.001$, $n = 48$, data not shown). Across all stations, the average NO_3:PO_4 ratio was a long way below Redfield (1958) at 4.2 ± 1.9. The average surface silicate concentrations had seasonal dynamics that were consistent with those for nitrate at both Port Hacking stations, but markedly different at Rottnest Island where silicate remained high throughout the year (Fig. 2E).

Stratification

The seasonal pattern of stratification was similar at all stations with a minimal difference in density between the surface and 50 or 100 m observed during mid-winter (Fig. 2C). The strength of stratification was similar for Rottnest and Maria Islands, but was up to 5 times greater at Port Hacking during late summer, mainly due to colder waters at depth. The seasonal weakening of stratification at Port Hacking was closely associated with a rise in the concentration of surface nitrate, suggesting a classic temperate zone mixing–light–nutrient control of the dominant phytoplankton responses.

SeaWiFS chl *a* (1997–2007)

All east coast stations showed seasonal chl *a* maxima in spring, with PH_{50m} having the greatest chl *a* concentrations (Fig. 2F), averaging 0.37 ± 0.11 mg m^{-3}. In contrast, chl *a* reached a maximum during winter at Rottnest Island, with concentrations <0.2 mg m^{-3} from September to April.

Phytoplankton

The phytoplankton results indicate considerable differences in the seasonal dynamics of community composition across sites (Fig. 2G). At Rottnest Island, there was little seasonality in the diatom:dinoflagellate ratio, which averaged 48% diatoms. Near Maria Island, the diatom:dinoflagellate ratio peaked in spring and midsummer. Unlike the other stations, at PH_{100m} the cell counts did not resolve any cells less than 35 µm (mesh size) and small cells of both taxa were not enumerated. Large diatoms tended to dominate the phytoplankton community at PH_{100m} with some dinoflagellates appearing in early summer.

Long-term changes in physicochemical parameters

There was a significant increase in average surface temperature at all stations with the greatest warming (2.02°C $century^{-1}$) at Maria Island and the lowest (0.74°C $century^{-1}$) at Port Hacking (Table 3). While all stations showed significant increases in surface temperature (Table 3), the rates of change were not uniformly distributed throughout the year (Fig. 2H). For example, at Maria Island in January the depth-averaged temperature increased ($p < 0.001$) fastest at 3.1 ± 0.4°C $century^{-1}$ (Fig. 2H). All stations showed significant warming during spring (September) and autumn (May), but no station showed a significant change in July. There were also long-term increases in surface salinity (ranging from 0.23 to 0.41 psu $century^{-1}$) at all 4 stations (Table 3). At Maria Island, long-term trends in stratification were not found in any month. At the other stations, trends in stratification were quite variable depending upon the month of the year (Fig. 2I). Significant long-term reductions in stratification were found for October at PH_{50m}, during March at PH_{100m} and in June and July at Rottnest Island. Significant long-term increases in stratification were limited to April, May and June at PH_{50m}. Surface nitrate concentrations increased significantly at PH_{100m} and Rottnest Island, at a rate of 0.56 and 0.40 µM $century^{-1}$, respectively. Surface phosphate concentrations also increased at all stations except PH_{100m} (Table 3). In strong contrast with phosphate and nitrate, all east coast sites showed a significant decline in surface silicate concentrations ranging from –2.3 to –5.8 µM $century^{-1}$. Two stations, PH_{50m} and Rottnest Island, also experienced long-term declines in surface dissolved oxygen concentrations (Table 3).

Detailed location-specific changes

Maria Island

Of all the stations, Maria Island experienced the greatest warming from 1944 to 2005 (Table 3), but the degree of stratification from 0 to 50 m did not change signifi-

Table 3. Long-term (>10 yr) linear trends in surface (0 m) ocean properties after seasonally detrending data by removing monthly means. Unless otherwise indicated, probabilities for all trends were <0.001; ns: not significant. The last row shows the linear regression results for surface July nitrate concentrations as a function of July surface temperature (as in Fig. 2I) with the intercept in brackets and slope italicised

	Maria Island	Port Hacking 100 m	Port Hacking 50 m	Rottnest Island
Maximum span (years analysed)	1944–2005	1953–2005	1944–2004	1951–2001
Maximum total no. observations[a]	3273	9263	9882	2736
Temperature (°C century^{-1})	2.02	0.746	0.744	1.23
Salinity (psu century^{-1})	0.346	0.232	0.269	0.407
Nitrate (µM century^{-1})	ns	0.556	ns	0.400 (p = 0.008)
Phosphate (µM century^{-1})	0.530	[c]	0.611[c]	0.313
Silicate[b] (µM century^{-1})	−5.84	−1.97	−2.30	ns
Dissolved oxygen (µM century^{-1})	ns	ns	−12.9	−49.1
Relationship between July temperature (°C) and July nitrate concentration (µM) at surface	*−1.04* (15.3) p < 0.004	*−0.31* (6.95) p < 0.001	*−0.45* (9.57) p < 0.001	*0.22* (−4.0) p = 0.048

[a]For any parameter. [b]Silicate measurements commenced in 1970 at all sites. [c]Gap in PO_4 measurements from 1985 to 2003

cantly in any month (Fig. 2I). At this station, the annual spring bloom occurred some 3 to 4 mo after the winter minimum in stratification (Fig. 3A), presumably due to the ~80 m deep mixed layer (Condie & Dunn 2006), producing a light-limited environment for phytoplankton growth (Sverdrup 1953). Mean depth-averaged annual nitrate concentrations (sampled monthly at 5 depths in the upper 50 m) have remained relatively constant over the last ~60 yr (Fig. 3D). In contrast, mean annual depth-averaged silicate concentrations have been highly variable since measurements started in 1970. Some of the variability appears associated with the SOI, with high silicate concentrations present just before or during high SOI years (Fig. 3D), but mean annual SOI was not correlated with silicate. Overall, there was a very strong downward trend in depth-averaged (0 to 50 m) silicate concentrations which reached an annual mean value of <0.6 µM in 2006, with the NO_3:Si molar ratio rising to 5.3 (Fig. 3D).

Near Maria Island, chl *a* concentrations were minimal during winter and rose in the spring to annual maxima in either September or October during 1997 to 2007 (Fig. 3A). Growth rates of this spring bloom have, however, declined steadily by ~8% per year (Fig. 3B; p = 0.004): they were 0.40 mo^{-1} in 1997 and fell to 0.17 mo^{-1} in 2006. This trend was robust whether growth rates were calculated over 3, 4 or 5 mo (from July to September, October or November, respectively, and across a much larger region, from 36 to 48° S by 152 to 167° E, Fig. 1). In addition, near Maria Island the peak in spring bloom biomass has been declining (p = 0.011) at about 6% yr^{-1} (Fig. 3C). This biomass response is in contrast to the average annual biomass across the majority of the Tasman Sea that has been increasing at a rate of 0.13 µg chl *a* l^{-1} decade^{-1} (1997 to 2007, p < 0.001). In the nearby Huon Estuary, there has been a strong rise in the peridinin:chl *a* ratio (= photosynthetic dinoflagellates:all phytoplankton) from 1997 to 2004 (Fig. 3E), while fucoxanthin : chl *a* (≈ diatoms:all phytoplankton) has remained relatively constant.

Port Hacking

The surface waters at PH_{50m} tended to be colder and less saline, with higher concentrations of nitrate, silicate and chl *a* (Fig. 2), and were generally less stratified than those at PH_{100m} (Fig. 2C). The long-term average oceanic warming at Port Hacking was less relative to other stations, with both PH_{50m} and PH_{100m} showing a modest but significant increase in temperature of ~0.7°C century^{-1} (Table 3). Long-term trends in salinity were ~0.25 psu century^{-1} at both PH_{50m} and PH_{100m} (Table 3), whereas changes in stratification were restricted to specific months. At PH_{50m}, stratification increased during autumn and early winter (April, May and June; p = 0.05, <0.001 and 0.027, respectively, Fig. 2I) and decreased in spring (p = 0.008). Further offshore, PH_{100m} showed a long-term decrease in stratification (p = 0.03), but only during March (Fig. 2I). PH_{100m} was the only station to show no long-term trend in surface phosphate concentration (Table 3). Surface nitrate concentrations showed a strong positive long term trend at PH_{100m}, but no significant trend was found at PH_{50m}. Silicate concentrations have fallen significantly at both stations over the past 60 yr at a rate of ~2 µM century^{-1}. Over all depths, the long-term average NO_3:Si molar ratios were 1.74 (n = 7761) and 1.79 (n = 4549) at PH_{100m} and PH_{50m}, respectively. Surface concentrations of dissolved oxygen declined significantly at PH_{50m}.

Temporally limited phytoplankton data from Port Hacking comprised two 1-yr data sets based on 35 µm

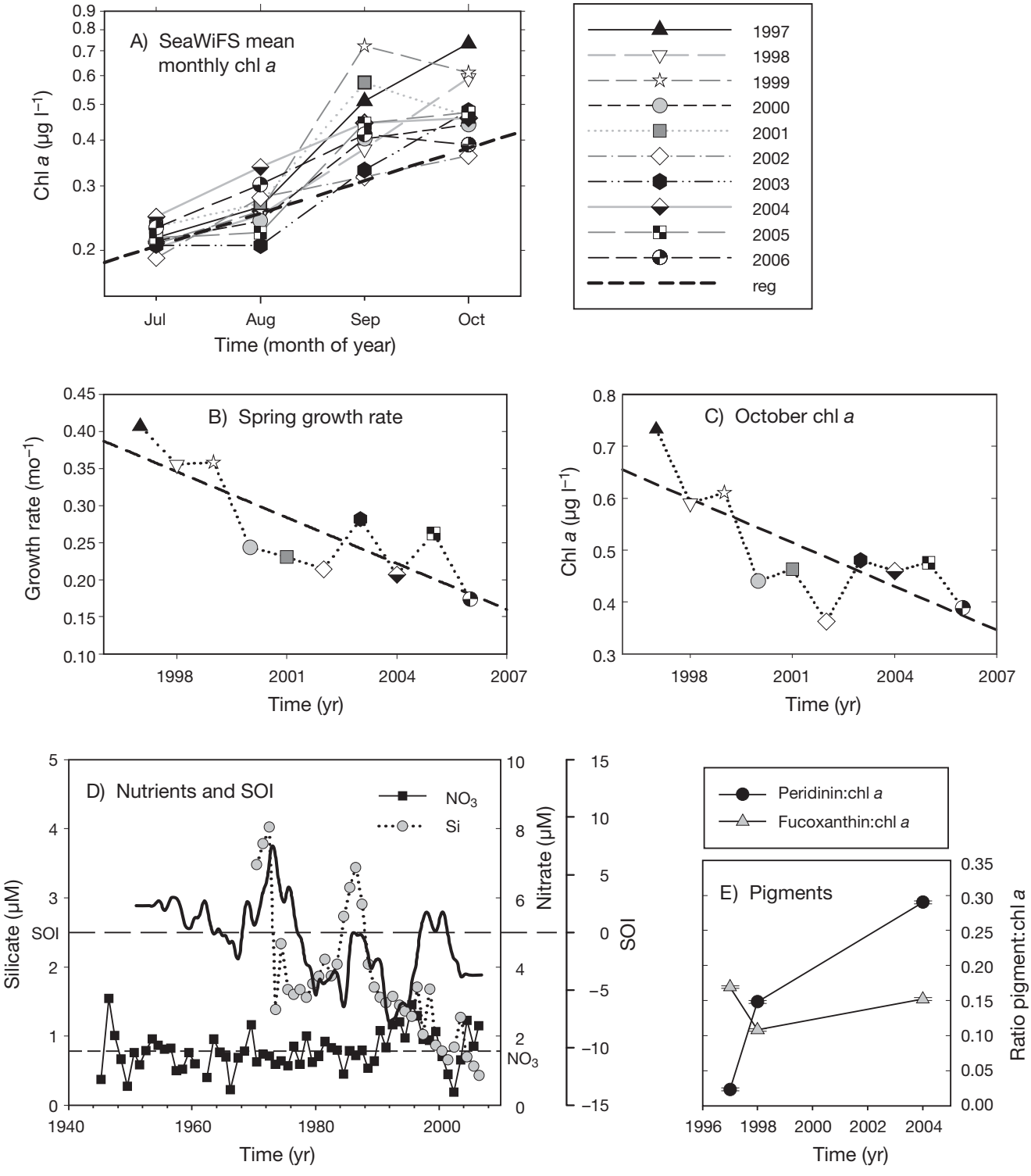

Fig. 3. (A) SeaWiFS monthly mean chlorophyll *a* (chl *a*) data from GIOVANNI over the area 42.2 to 43.0° S by 148.2 to 149.0° E. For each year, a growth rate was estimated from the regression of $\log_e$ chl *a* versus time; a single example is shown for 2002. (B) Spring chl *a* growth rates calculated from data in (A); dashed line is regression ($p = 0.004$). (C) Monthly mean chl *a* concentrations; dashed line is regression ($p = 0.011$). (D) Data for nutrients at Maria Island, 42.5° S and 148.1° E, from 1944 to 2005 at 0, 10, 20, 30, 40 and 50 m depth. Short dashed line is long-term mean nitrate concentration; long dashed line is zero Southern Oscillation Index (SOI). (E) Pigment data from 3 locations ~43.3° S and 147.1° E, sampled by 12 m integrated tube during 1996–1998 and 2004–2005, n = 359. Annual mean and SE are shown

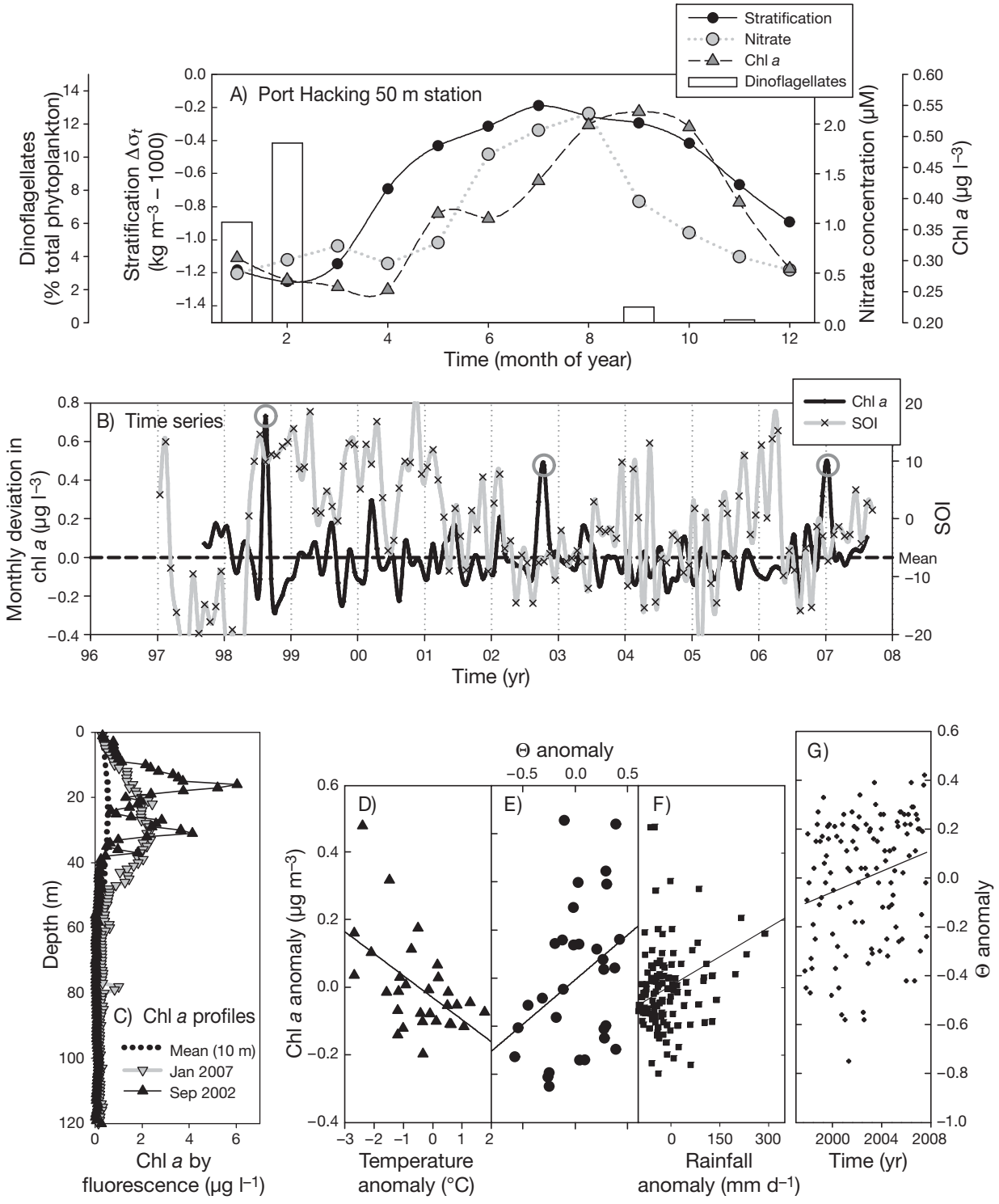

Fig. 4. Port Hacking physical (as in Table 1) and chlorophyll *a* (chl *a*) data (from GIOVANNI) over the period September 1997 to September 2007 (see Table 2, Fig 1). (A) Port Hacking 50 m long-term (1944–2005) mean monthly surface nitrate concentrations and stratification ($\Delta\sigma_t$) at the surface minus density at 50 m. (B) Chl *a* deviations from monthly means versus time (dashed line is long-term mean), Southern Oscillation Index (SOI) versus time. Open grey circles indicate substantial and anomalous bloom events. (C) Vertical profiles of fluorescence from Port Hacking 100 m station, long-term mean (10 m averaged) and 2 bloom events (1 m averages). Correlations of (D) Port Hacking 100 m: temperature anomaly against SeaWiFS-derived chl *a* anomaly in summer (n = 30, p = 0.002), (E) Port Hacking 100 m: fraction of East Australian Current (EAC) water (Θ_{100}) anomaly with chl *a* anomaly in winter (n = 30, p = 0.03) and (F) Port Hacking 50 m: monthly rainfall anomaly with chl *a* anomaly (n = 120, p = 0.0004). (G) Regression showing an increasing fraction of EAC waters at Port Hacking 100 m station over the last decade, which suggests a 21 ± 9% increase in the fraction of EAC water at Port Hacking from September 1997 to September 2007 (n = 120, p = 0.01)

mesh net tows (Hallegraeff 1981, Ajani et al. 2001) and did not allow an analysis of long-term changes in phytoplankton biomass or species composition. Based on these limited data, the phytoplankton at PH_{50m} were diatom-dominated with the dinoflagellates reaching their greatest proportion of the community (~11% of cells) during February (Figs. 2G & 4A), the time of maximum stratification.

SeaWiFS chl *a* anomalies (observations minus monthly mean) showed substantial (~+100% of monthly mean) episodic blooms (Fig. 4B). In the last 10 yr, the largest of these occurred in August 1998, October 2002 and January 2007 (circled peaks in Fig. 4B). There were vertical profiles of fluorescence for 2 of these anomalous blooms that show substantial chl *a* over depths from 10 to 50 m (Fig. 4C). Depth-integrated chl *a* (fluorometer inferred) in these blooms ranged up 93 mg m^{-2} (January 2007) or about 3 times the long-term depth-averaged value (~30 mg m^{-2}). Unlike Rottnest Island, the pattern of these anomalies was not correlated with simultaneous SOI values; however, when lagged 4 mo, the SOI versus chl *a* relationship was significant ($p = 0.016$). The time series (Fig. 4B) is suggestive of a trend for blooms to be associated with the transition from negative to positive SOI. Such transitions often bring rainfall to southeast Australia (Cai & Cowan 2008), and monthly SeaWiFS chl *a* anomalies at Port Hacking were strongly and positively correlated with Sydney rainfall (Fig. 4F, $n = 120$, $p < 0.001$).

Some factors influencing phytoplankton dynamics were only seasonal, such as the strong negative correlations between the chl *a* anomaly and SOI and temperature during summer (Table 4, Fig. 4D). The negative, non-significant correlation of chl *a* with southward alongshore winds ($R = -0.32$, Table 4), and a weak, non-significant positive correlation with Θ_{100} ($R = 0.16$) indicates that the summer temperature anomaly was due to upwelling-favourable winds rather than northward transport of cool Tasman Sea surface waters (the latter would have produced a negative correlation with Θ_{100}). The SOI index did not correlate significantly with chl *a* anomalies in the other seasons. The Θ_{100} index was positively correlated (=stronger EAC) with SeaWiFS chl *a* near Port Hacking in the late autumn-early winter months (May to July, Table 4, Fig. 4E). Of the Port Hacking physical indices, the strongest trend over the last decade was the increasing fraction of EAC water or Θ_{100} (Fig. 4G), which suggests a strengthening of the poleward extension of the EAC as predicted by global climate models (Cai 2006).

Table 4. Seasonally grouped correlation coefficients (R) of physical indices versus SeaWiFS-derived monthly chlorophyll *a* anomalies at the Port Hacking 100 m station (monthly mean values from September 1997 to September 2007, n = 30 per season). Θ_{100}: fraction of East Australian Current water (see Appendix 1 for details); SOI: Southern Oscillation Index. Bold plus italic values are significant at $p < 0.05$ while bold values are significant at $p < 0.01$. Wind speed data based on US National Center for Atmospheric Research ¼ degree 6 hourly reanalysis (Kalnay et al. 1996)

Season	Temperature	Alongshore wind	Wind speed	Θ_{100}	SOI
Nov–Jan	**–0.53**	–0.32	0.05	0.16	***–0.57***
Feb–Apr	–0.01	–0.02	0.12	–0.27	0.10
May–Jul	***0.36***	–0.14	–0.24	***0.40***	–0.19
Aug–Oct	0.21	–0.18	***0.43***	–0.02	–0.01

Rottnest Island

The ocean at Rottnest Island has become warmer and more saline, with higher nitrate, phosphate and lower oxygen concentrations, on average, over time (Table 3). It has also become less stratified during winter ($p = 0.003$, $p < 0.001$, for June and July, respectively, Fig. 2I). Surface nitrate concentrations at Rottnest Island tended to be variable with near-zero values recorded in every month of the year (Fig. 5A). In spite of the high temporal variability, there was a seasonal trend and fitting the data to a Gaussian curve showed a significant ($p < 0.0001$, $n = 462$) rise to ~0.7 µM in June. Silicate concentrations showed less seasonal variation than nitrate (data not shown) and no interannual trend (Table 3) or correlation with SOI (data not shown). Over the 31 yr between 1970 and 2002, silicate concentrations (0 to 50 m) were high relative to other coastal stations, averaging 2.28 µM. The mean nitrate concentration (0 to 50 m) was 0.59 µM, giving an average NO_3:Si molar ratio of 0.26. The seasonal peak in surface nitrate was consistent with the minimum in stratification that also occurred in June (Figs. 2C,D & 5A). Unlike the other stations, however, there was no temporal offset between the seasonal minimum in stratification and annual maximum in chl *a*.

The phytoplankton biomass across most of southwestern Australia (28° to 34° S by 114° E to shore; Fig. 1) showed a positive correlation between annual chl *a* anomalies and mean SOI. For example, in the region from 31° to 33° S by 114° E to 115° E (Fig. 1), annual chl *a* anomalies were correlated with SOI ($p = 0.027$, Fig. 5B). The linear relationship between SOI and chl *a*, although somewhat dependent upon the exact region selected, tended to be even stronger if only negative SOI years were included ($p = 0.009$, Fig. 5B). Positive SOI years (1999, 2000) showed greater than normal chl *a* concentrations (Fig. 5B) and this was most evident during summer and autumn (Fig. 5C). Anomalies were calculated as the deviations from the 8 d average chl *a* concentrations fit to a Gaussian model; the

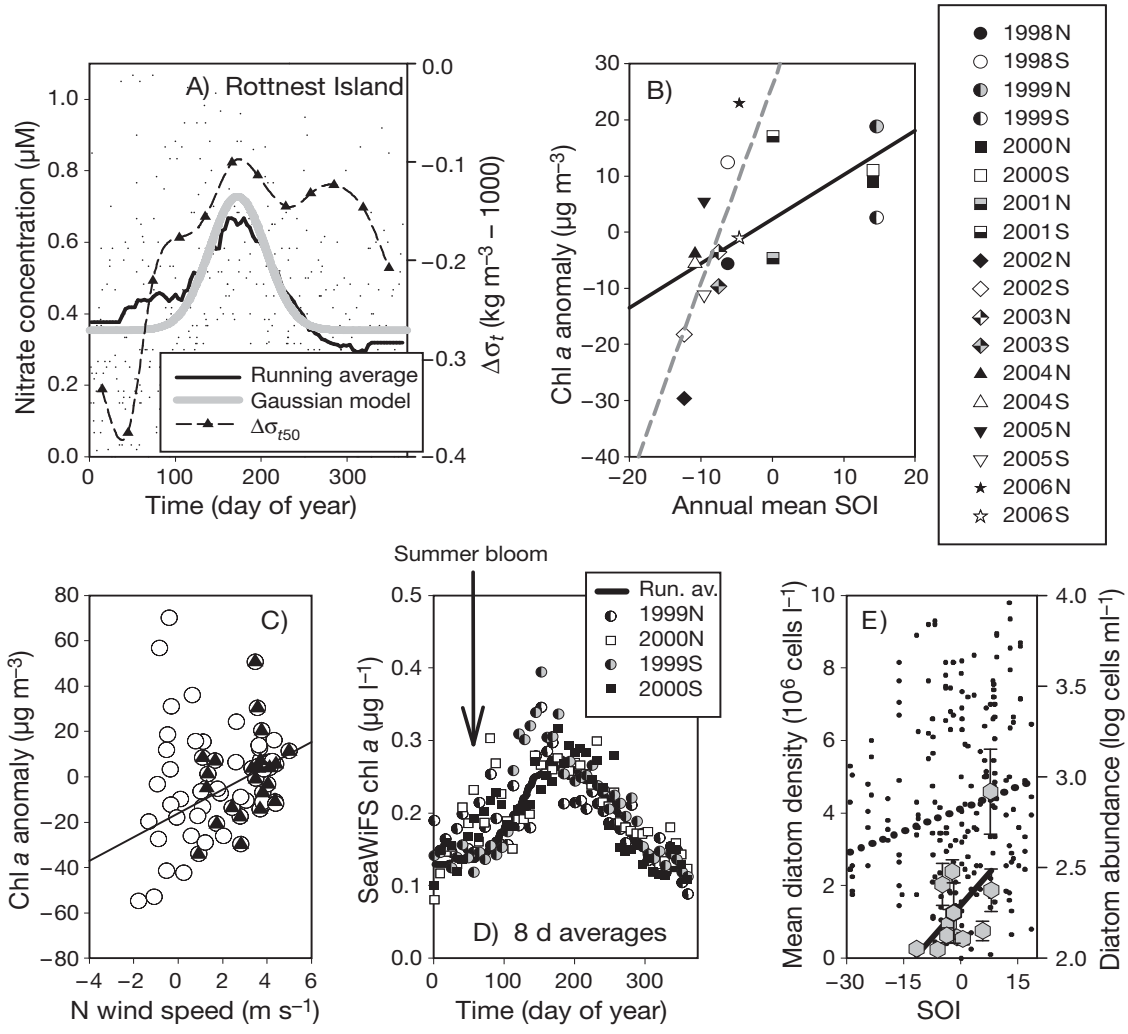

Fig. 5. Rottnest Island (32.0° S, 115.4° E) data sampled at 0, 10, 20, 30, 40 and 50 m ca. monthly from 1951 to 2001 (see Table 1 for details). (A) Nitrate concentrations (small dots), running average (solid black line), Gaussian model fit to data (thick grey line) and mean monthly stratification at the surface minus density at 50 m (▲; $\Delta\sigma_{t50}$). (B) Annual chlorophyll *a* (chl *a*) deviations from mean concentrations estimated from SeaWiFS NASA GIOVANNI over the period from September 1997 to September 2007 plotted against the Southern Oscillation Index (SOI). S: south; N: north (see Fig. 1). Solid line is regression through all data (p = 0.027); dashed line is through negative SOI values only (p = 0.007). (C) Monthly mean north (positive values are from the south) wind speed from GIOVANNI MERRA at 10 m over 30 to 36° S by 110 to 120° E from 1997 to 2007 versus monthly chl *a* anomaly; (O) all data (p = 0.13); (▲) summer only (p = 0.07, solid line). (D) SeaWiFS chl *a* data for La Niña years; solid line is long-term running average. (E) Diatom abundance at nearby site versus SOI. Large symbols are monthly mean diatom cell densities (left-hand *y*-axis) for weekly observations from February in each year (1994 to 2007); error bars are SD; solid line is regression (p = 0.034). Small symbols are weekly samples (right-hand *y*-axis) for January to April from 1994 to 2007; dotted line is regression (p = 0.012)

anomalies were significantly ($p < 0.001$) correlated with SOI values (data not shown). There were no negative chl *a* anomalies associated with predominately northerly winds (Fig. 5C), although the overall correlation was weak (p = 0.13), albeit slightly stronger in summer (p = 0.07). Monthly mean $\log_{10}$ diatom abundance in February showed a strong relationship (p = 0.034) with annual mean SOI (Fig. 5E). Similarly, weekly samples from January to April also showed a significant (p = 0.012) relationship between $\log_{10}$ diatom abundance and monthly mean SOI.

DISCUSSION

Long-term changes in ocean properties and their implications for phytoplankton

Climate change impacts cannot be detected without long-term observations because oceanic properties, including phytoplankton biomass, vary significantly across a range of spatial and temporal scales (Platt & Denman 1975). Our analysis of ~60 yr of observations from 4 coastal stations detected long-term changes in

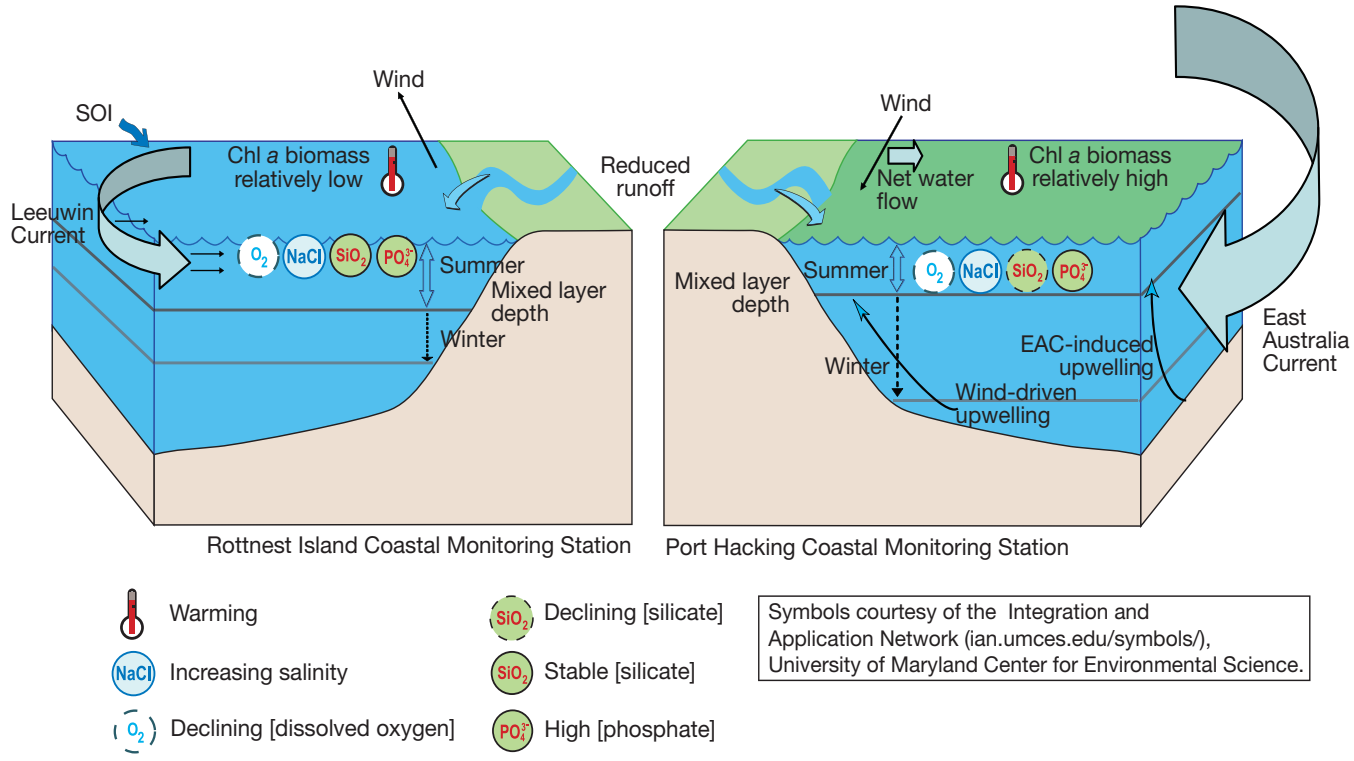

Fig. 6. Conceptualization of the oceanic properties and their long-term trends on the west and east coasts of Australia in the vicinity of Rottnest Island and Port Hacking (50 m), respectively. Current arrow size indicates relative volume of flow. SOI: Southern Oscillation Index; EAC: East Australian Current. Locations are identified in Fig. 1; statistical analysis of trends can be found in Table 3

surface temperature, salinity and dissolved nutrients that have the potential to impact phytoplankton production and species composition (conceptualized in Fig. 6). The rates of change in temperature identified in the present study are consistent with those from other oceanographic regions (Levitus et al. 2005), with greatest increase at Maria Island in the western Tasman Sea, a body of water known to be warming quickly (Ridgway 2007). On average, stations showed their greatest long-term temperature changes during spring and autumn, effectively lengthening the phytoplankton growing season. Changes in salinity, while statistically significant, are probably not of sufficient magnitude to have a direct impact on phytoplankton growth rates or the resulting community composition. They do, however, indicate changes in the oceanic environment arising from a range of potential location-specific mechanisms (see below) that could indirectly impact on phytoplankton.

In contrast to modelling studies, which predict a 5% decrease in global ocean productivity due to the reduced vertical transfer of nutrients (Cox et al. 2000, Bopp et al. 2001), the present study shows little evidence of increasing vertical stratification, except at PH_{50m} where it was limited to April, May and June (late autumn-early winter). The other 3 stations showed declines in stratification at various times of the year. Importantly, there was no indication of a decline in mid-winter nitrate concentrations or surface temperatures. A decline in vertical mixing has been inferred as the cause of decreases in subsurface concentrations of dissolved oxygen concentrations in most of the world's oceans (Plattner et al. 2002); however, the declines in surface dissolved oxygen observed at Port Hacking and Rottnest Island are unlikely to imply a decline in vertical mixing. They may reflect changes in oxygen solubility, horizontal transport of low dissolved oxygen waters or a shift in the ratio of remineralization of organic matter relative to primary production. At present there are limited data to distinguish the likelihood of these alternatives, but a more rapid organic matter decay associated with warmer temperatures is suggested.

The finding of greatest significance for phytoplankton production in the present study is the long-term decrease in dissolved silicate concentrations in east coast waters, reaching annual mean concentrations at Maria Island below the half saturation value for diatom uptake, potentially restricting their growth (Paasche 1973). Even in the 1960s, low silicate was proposed to

limit diatoms on the east coast of Australia (Grant 1971), but the concentrations have declined significantly since then; by 2006 the NO_3:Si ratios at Maria were 5 times the expected Redfield ratio of ~1 (Redfield 1958). Clearly, silicate, rather than nitrate, will increasingly become the limiting nutrient in these waters. Thus we anticipate shifts in east coast diatom species, long-term declines in east coast diatoms as a proportion of the total phytoplankton community (e.g. Edwards et al. 2001) and a reduction in primary productivity if the decline in silicate concentrations continues. The availability of silicate is also strongly linked with vertical carbon flux (leading to deep ocean carbon sequestration), to such an extent that variation in silica supply is suggested as the cause of the 40% reduction in pCO_2 during the last interglacial period (Harrison 2000).

All stations showed a significant change in at least one ocean property, but the patterns were not always consistent between sites, even at PH_{50m} and PH_{100m} which are only ~3 km apart. Oceanographic conditions at PH_{50m} tended to be colder and less saline, with greater concentrations of nitrate, silicate and chl *a* than those at PH_{100m}, indicating steep onshore–offshore gradients along this section of coast with its relatively narrow continental shelf. Both Port Hacking stations showed significant trends of increasing salinity and decreasing silicate and in both cases the rates of change were greater nearshore. In addition, both stations exhibited warming, but only PH_{50m} had significant long-term trends in concentrations of phosphate and dissolved oxygen. The ~10 yr longer time series at PH_{50m} contributes to the trend for increasing phosphate as the lowest concentrations were observed in the 1940s. The downward trend in dissolved oxygen at PH_{50m} and not PH_{100m} might reflect the greater degree of benthic–pelagic coupling nearshore and the temperature-dependent recycling of organic matter.

The majority of data used in the present study arose from a monitoring design conceived in the 1940s. After >60 yr, it is evident that the physical and chemical data collected at approximately monthly intervals and vertically at approximately 10 m intervals were adequate for the description of long-term trends. They were also adequate to resolve seasonal dynamics. The amount of biological sampling was more limited and indicates the need for more frequent observations and greater depth resolution to adequately characterize plankton responses, particularly in view of satellite sensors that cannot detect subsurface (>20 m) chl *a* distributions. In addition, there are >10 phytoplankton bioregions proposed for the regional seas of Australia (Hayes et al. 2005), suggesting significantly more monitoring stations are needed to characterize these. Regardless of the limitations of the sampling, the data suggest that variation in the boundary currents around Australia, the Leeuwin Current and the EAC, are the primary factors determining the change in shelf-scale biological oceanography. These large oceanic currents transport planktonic species plus their pelagic habitat including heat, salt and nutrients southwards on both coasts. On the eastern Australian coast, the strengthening EAC (Ridgway 2007, Hill et al. 2008) is extending the distribution and abundance of some planktonic species. For example, in the 1950s the heterotrophic dinoflagellate *Noctiluca scintillans* was reported to have a strong presence in Moreton Bay (Wood 1954, 1964) and then large blooms were observed off NSW in the 1990s (Ajani et al. 2001, Dela-Cruz et al. 2002, 2003). In 2002, *N. scintillans* arrived in SE Tasmania where it is now the dominant mesoplanktor (Thompson et al. 2008); a journey of ~2000 km over ~50 yr.

Maria Island

At Maria Island, the seasonal phytoplankton dynamics are determined by wind- and temperature-driven mixing and consequent nutrient input into surface waters during winter (Harris et al. 1987), with the peak of the spring bloom some 3 mo later. Mesoscale variation in the front between EAC and subantarctic waters also contributes significantly to the seasonal and interannual variation in nutrient concentrations (Harris et al. 1987). Over the ~30 yr record analysed here, the dissolved silicate concentrations have fallen precipitously, such that in 2006 the average NO_3:Si molar ratio at Maria Island was well below Redfield (1958) and substantially lower than the other Australian coastal stations. Several mechanisms could be responsible for the decline in surface silicate: the reduction in regional rainfall and runoff, a reduction in the upwards flux of dissolved nutrients, an increase in the downwards flux of particulate Si, or the increased poleward transport of lower nutrient (silicate) surface waters. Previous work has shown the EAC is strengthening and intruding further south (Ridgway 2007, Hill et al. 2008). We therefore hypothesize that the poleward transport of this relatively warm, low silicate water along the western edge of the Tasman Sea is the primary cause for the decline in silicate concentrations at Maria Island and at Port Hacking. From 1997 to 2007, the spring bloom biomass (chl *a*) at Maria Island has decreased by ~50% as has its growth rate. This decline could be an artifact of the surface bias of remotely sensed chl *a*, possibly an increase in the average depth of the chl *a*. If true it would still imply a substantial change in the phytoplankton ecology of the region. In the Ligurian Sea, a similar decline in silicate was associated with a

decline in the fast-growing diatoms within the spring bloom (Goffart et al. 2002). Thus at Maria Island the dramatic fall in silicate concentrations may explain the slower development of the spring bloom and the regional shift towards dinoflagellates. In waters close to Maria Island, the diatom *Skeletonema* spp., with its low half-saturation constant for Si uptake (Paasche 1973), has replaced a range of *Pseudo-nitzschia* species as the dominant diatom taxon (Thompson et al. 2008) while dinoflagellates have increased (present study). A similar shift in flora towards dinoflagellates has been observed in continuous plankton recorder data from the North Atlantic (Edwards & Richardson 2004), but insufficient data were available to investigate whether the cause was a reduction in surface dissolved silicate concentrations. Importantly, dinoflagellates often have inferior nutritional values in phytoplankton–copepod–fish food webs relative to diatoms (McQuatters-Gollop et al. 2007), and their increasing dominance could have profound implications for fisheries production.

Port Hacking

In general, El Niño conditions (negative SOI) in southeastern Australia are associated with warmer waters, lower nutrient concentrations (Lee et al. 2001) and reduced temperature stratification (Lee et al. 2007). As a result of the Ekman transport associated with the southward flow of the EAC, the continental shelf along the NSW coast has cold, nutrient-rich water relatively close to the surface (Baird et al. 2006). During summer, when the EAC flow is faster, this cold, nutrient-rich water is much closer to the surface than at the other coastal stations. The shallow depth of this nutrient source means less energy is required to transport it into the euphotic zone, making this region susceptible to nutrient enrichment due to upwelling triggered by relatively weak physical forcing. The intrusions of deeper water onto the shelf results from 4 different mechanisms: (1) wind-driven upwelling, (2) upwelling due to the EAC intruding onto the shelf, (3) acceleration of the EAC as the shelf narrows and (4) separation of the EAC from the coast (McLean-Padman & Padman 1991, Roughan & Middleton 2002). Frequently, upwelling occurs north of Port Hacking, often at ~31°S (Rochford 1975, Tranter et al. 1986, Cresswell 1994, Gibbs et al. 1997, Oke & Middleton 2001) and, as shown in the present study, the resulting phytoplankton bloom is subsurface by the time it arrives at Port Hacking (~34°S). These upwelling-favourable conditions are known to have a link with SOI atmospheric (Hsieh & Hamon 1991) and local weather conditions (McLean-Padman & Padman 1991). The strong negative summer correlations between SOI and temperature with the chl *a* anomaly indicate more phytoplankton biomass is present in summers when more cold water is pushed into the coastal zone, probably due to upwelling-favourable winds. In late autumn and early winter (May to July), a relatively strong EAC and warmer conditions were associated with more chl *a* as the cooling and deep mixing that would normally restrict primary production and result in a sharp, winter decline in chl *a* were reduced. More chl *a* in spring was positively correlated with wind speed, indicating an association with vertical mixing. The strongest trend over the last decade at Port Hacking was the increasing fraction of EAC water (Θ_{100}). This indicates a strengthening of the poleward extension of the EAC as predicted by global climate models (Cai 2006), encouraging us to predict continued increases in chl *a* during late autumn and early winter. Periodic algal blooms have been reported since the 1960s (Humphrey 1963, Hallegraeff & Reid 1986, Pritchard et al. 2003), and SeaWiFS data showed 3 large chl *a* anomalies at Port Hacking between 1997 and 2007. The previous blooms have been largely diatom-dominated and 1997–1998 samples indicated a general dominance by diatoms with dinoflagellates becoming relatively more abundant during late summer. While no long-term trends in phytoplankton abundance or composition were detected, the increasing strength of the EAC, a strong warming trend in autumn and low and declining silicate concentrations (Grant 1971, present study) suggest the autumn bloom will contain an increasing component of flagellates.

Rottnest Island

On the west coast of Australia, the poleward-flowing Leeuwin Current delivers its peak volume of warm, relatively silicate-rich water in mid-winter (Feng et al. 2003), reducing the capacity of convective cooling to deepen the surface mixed layer. As a result, the winter mixed layer depths are considerably less than on the east coast of Australia (40 to 60 m as opposed to >75 m; Condie & Dunn 2006). The presence of Leeuwin Current water reduces stratification over 0 to 50 m (e.g. at Rottnest Island) and is associated with a shelf-scale, mid-winter phytoplankton bloom. The strong association between SOI and chl *a* concentrations (present study) suggests more nutrients are injected into the surface mixed layer in weak El Niño or La Niña years. This could be due to the increased strength of the Leeuwin Current (Feng et al. 2003), but the major phytoplankton anomalies (an increase in chl *a* biomass and a greater proportion of diatoms) were associated with a positive SOI and occurred during late summer

when the Leeuwin Current was relatively weak. We propose that this anomalous summer bloom arises in the more productive (Hanson et al. 2005) northward flowing and predominantly summer Capes Current (Pearce & Pattiaratchi 1999). We propose that summer La Niña atmospheric conditions produce a stronger Capes Current due to the anomalous low pressure over northwestern Australia that increases the frequency of northward winds (c.f. Jones & Trewin 2000, their Fig. 3). The Capes Current flows landward of the Leeuwin Current and brings colder and more nutrient-rich water into the euphotic zone of the nearshore region in the southwest (Gersbach et al. 1999). Based on unpublished current meter data (G. Cresswell pers. comm.), these winds result in more Capes Current water being transported substantially further north. This nutrient supply mechanism may explain some of the cross-shelf variability observed in phytoplankton biomass in the southwest region (Pearce et al. 2006).

Mechanisms of change in ocean properties

The increased salinities observed at Australian temperate coastal stations could arise from increased transport of relatively high salinity water southwards by the EAC and Leeuwin Current along east and west coasts, respectively. Both currents are, however, relatively fresh closer to the tropics (Feng et al. 2003, Boland & Church 1981, respectively). Thus increased evaporation in these currents as they move southwards is more likely to explain this trend. At latitudes of 15 to 30°, the global ocean has greater surface salinity due to high net evaporation (Levitus et al. 1994, Condie & Dunn 2006) in association with atmospheric Hadley cells (Baumgartner & Reichel 1975, Schmitt et al. 1989). In addition, some component of the increased salinity along temperate Australian coasts must be associated with the long-term (>10 yr) drying trend across temperate latitudes in terrestrial Australia (Timbal et al. 2006), resulting in higher evaporation and lower freshwater runoff. The net increase in salinity at Rottnest Island is equivalent to a decline of 0.6 m of freshwater being mixed into the upper 50 m of the ocean. Such a result is consistent with the well-documented 41 yr drying trend of ~0.7 mm yr^{-1} observed in SW Australia since 1958 (Timbal 2004, Timbal et al. 2006). Similarly, the decline in precipitation over eastern Australia (Cai & Cowan 2008) could be responsible for a portion of the increasing salinity at Port Hacking and Maria Island. Thus reduced freshwater input and increased evaporation and transport (e.g. Feng et al. 2003, Ridgway 2007, Hill et al. 2008) could be driving salinity changes in Australian coastal waters.

We propose that the east coast decline in surface silicate is due to a change in the long-term supply from southward-flowing EAC water (Ridgway 2007, Hill et al. 2008). We speculate that the warm (buoyant) EAC waters are progressively stripped of dissolved silicate by diatoms during its southward transport. The silica is exported from surface waters as particulate silica (Kamykowski et al. 2002), while a greater portion of N and P are remineralized. Increased poleward transport by strengthening temperate gyres could make this mechanism a potential threat to diatom-based production in all temperate zones (e.g. Behrenfeld et al. 2006), a suggestion that is consistent with phytoplankton observations in the North Atlantic (Edwards & Richardson 2004).

CONCLUSIONS

Climate models predict that the ocean's physical circulation and chemical properties will shift significantly in the coming decades, affecting phytoplankton production and floristics (Boyd et al. 2008). Our analysis of long-term coastal data sets demonstrates changes have already occurred in a range of ocean properties within Australia's continental shelf waters. For most properties, the magnitude of change varied by season and the timing has important implications for the biological responses. Changes such as stratification and surface nutrient and chl *a* concentrations at the 4 Australian coastal stations were not consistent with predictions by existing spatially coarse, global climate change models, indicating the need for greater emphasis on regional observation and interpretation. Only with improved observations can we hope to link local- and regional-scale environmental changes with their biological responses. Achieving this level of observation is a significant challenge for the marine science community, but necessary if we wish to understand the impacts of climate variability and the consequent implications for our marine ecosystems.

Acknowledgements. Many people have been involved in maintaining the time series at these 4 coastal monitoring stations, now part of Australia's Integrated Marine Observing System (IMOS) — they are all sincerely thanked. Thanks to G. Cresswell, M. Feng and A. Waite and 2 anonymous reviewers for their constructive inputs. We are most appreciative to the Department of Water and Swan River Trust for West Australian phytoplankton data, P. Bonham (CSIRO) for Tasmanian pigment and phytoplankton data and P. Ajani (NSW EPA) for Port Hacking phytoplankton data. This research was supported by the CSIRO Wealth from Oceans Flagship Program and the NSW Department of Environment and Climate Change. This is SIMS contribution no. 0031.

LITERATURE CITED

Ajani PA, Lee RS, Pritchard TR, Krogh M (2001) Phytoplankton patterns at CSIRO's long-term coastal station off Sydney. J Coast Res 34:60–73

Armstrong FAJ (1951) The determination of silicate in sea water. J Mar Biol Assoc UK 30:149–160

Baird ME, Timko PG, Suthers IM, Middleton JH (2006) Coupled physical–biological modelling study of the East Australian Current with idealised wind forcing. I. biological model intercomparison. J Mar Syst 59:249–270

Baumgartner A, Reichel E (1975) The world water balance: mean annual global, continental and maritime precipitation. Elsevier, Amsterdam

Beaugrand G (2004) The North Sea regime shift: evidence, causes, mechanisms and consequences. Prog Oceanogr 60: 245–262

Behrenfeld MJ, Malley RTO, Siegel DA, McClain CR and others (2006) Climate-driven trends in contemporary ocean productivity. Nature 444:752–755

Boland FM, Church JA (1981) The East Australian Current 1978. Deep-Sea Res A 28:937–957

Bopp L, Monfray P, Aumont O, Dufresne JL and others (2001) Potential impact of climate change on marine export production. Global Biogeochem Cycles 15:81–99

Boyd PW, Doney SC, Strzepek R, Dusenberry J, Lindsay K, Fung I (2008) Climate-mediated changes to mixed-layer properties in the Southern Ocean: assessing the phytoplankton response. Biogeosciences 5:847–864

Cai WJ (2006) Antarctic ozone depletion causes an intensification of the Southern Ocean super-gyre circulation. Geophys Res Lett 33, L03712, doi:10.1029/2005GL024911

Cai WJ, Cowan TD (2008) Dynamics of late autumn rainfall reduction over southeastern Australia. Geophys Res Lett 35, L09708, doi:10.1029/2008GL033727

Chassot E, Mélin F, Le Pape O, Gascuel D (2007) Bottom-up control regulates fisheries production at the scale of ecoregions in European seas. Mar Ecol Prog Ser 343:45–55

Condie SA, Dunn JR (2006) Seasonal characteristics of the surface mixed layer in the Australasian region: implications for primary production regimes and biogeography. Mar Freshw Res 57:569–590

Cowley R, Critchley G, Eriksen R, Latham V, Plaschke R, Rayner M, Terhell D (1999) Hydrochemistry operations manual. CSIRO Marine Laboratories Report No. 236. CSIRO Marine Research, Melbourne

Cox PM, Betts RA, Jones CD, Spall SA, Totterdell IJ (2000) Acceleration of global warming due to carbon-cycle feedbacks in a coupled climate model. Nature 408:184–187

Cresswell GR (1994) Nutrient enrichment of the Sydney continental shelf. Aust J Mar Freshw Res 45:677–691

Cushing DH (1974) The natural regulation of fish populations. In: Harden Jones FR (ed) Sea fisheries research. Elek Science, London, p 399–412

Dela-Cruz J, Ajani P, Lee R, Pritchard T, Suthers I (2002) Temporal abundance patterns of the red tide dinoflagellate *Noctiluca scintillans* along the southeast coast of Australia. Mar Ecol Prog Ser 236:75–88

Dela-Cruz J, Middleton J, Suthers IM (2003) Population growth and transport of the red tide dinoflagellate, *Noctiluca scintillans*, near Sydney, Australia, using cell diameter as a tracer. Limnol Oceanogr 48:656–674

Edwards M, Reid PC, Planque B (2001) Long-term and regional variability of phytoplankton biomass in the Northeast Atlantic (1960–1995). ICES J Mar Sci 58:39–49

Edwards M, Richardson AJ (2004) Impact of climate change on marine pelagic phenology and trophic mismatch. Nature 430:881–884

Falkowski PG, Raven JA (2007) Aquatic photosynthesis. Princeton University Press, Princeton, NJ

Fofonoff NP (1985) Physical properties of seawater: a new salinity scale and equation of state for seawater. J Geophys Res 90:3332–3342

Feng M, Meyers GA, Pearce AF, Wijffels SE (2003) Annual and interannual variations of the Leeuwin Current at 32° S. J Geophys Res 108:1–19

Gersbach GH, Pattiaratchi CB, Ivey GN, Cresswell GR (1999) Upwelling on the south-west coast of Australia—source of the Capes Current. Cont Shelf Res 19:363–400

Gibbs MT, Marchesiello P, Middleton JH (1997) Nutrient enrichment of Jervis Bay, Australia, during the massive 1992 coccolithophorid bloom. Mar Freshw Res 48:473–478

Goffart A, Hecq JH, Legendre L (2002) Changes in the development of the winter-spring phytoplankton bloom in the Bay of Calvi (Northwestern Mediterranean) over the last two decades: a response to changing climate? Mar Ecol Prog Ser 236:45–60

Grant BR (1971) Variation in silicate concentration at Port Hacking station, Sydney, in relation to phytoplankton growth. Aust J Mar Freshw Res 22:49–54

Gregg WW, Casey NW, McClain CR (2005) Recent trends in global ocean chlorophyll. Geophys Res Lett 32, L03606, doi:10.1029/2004GL021808

Hallegraeff GM (1981) Seasonal study of phytoplankton pigments and species at a coastal station off Sydney: importance of diatoms and the nanoplankton. Mar Biol 61: 107–118

Hallegraeff GM, Jeffrey SW (1993) Annually recurrent diatom blooms in spring along the New South Wales coast of Australia. Aust J Mar Freshw Res 44:325–334

Hallegraeff GM, Reid DD (1986) Phytoplankton species successions and their hydrological environment at a coastal station off Sydney. Aust J Mar Freshw Res 37:361–377

Hanson CE, Pattiaratchi CB, Waite AM (2005) Seasonal production regimes off south-western Australia: influence of the Capes and Leeuwin Currents on phytoplankton dynamics. Mar Freshw Res 56:1011–1026

Harris G, Nilsson C, Clementson L, Thomas D (1987) The water masses of the east coast of Tasmania: seasonal and interannual variability and the influence on phytoplankton biomass and productivity. Aust J Mar Freshw Res 38: 569–590

Harrison KG (2000) Role of increased marine silica input on paleo-pCO_2 levels. Paleoceanography 15:292–298

Hayes D, Lyne V, Condie S, Griffiths B, Pigot S, Hallegraeff G (2005) Collation and analysis of oceanographic datasets for the National Marine Bioregionalisation. National Oceans Office Report. Department of the Environment and Heritage, CSIRO Marine Research, Melbourne

Hays GC, Richardson AJ, Robinson C (2005) Climate change and marine plankton. Trends Ecol Evol 20:337–344

Hill KL, Rintoul SR, Coleman R, Ridgway KR (2008) Wind forced low frequency variability of the East Australia Current. Geophys Res Lett 35, L08602, doi:10.1029/2007GL032912

Hsieh W, Hamon BV (1991) The El Niño-Southern Oscillation in south-eastern Australian waters. Aust J Mar Freshw Res 42:263–275

Humphrey GF (1963) Seasonal variations in plankton pigments in waters off Sydney. Aust J Mar Freshw Res 14:24–36

Jitts HR (1965) The summer characteristics of primary productivity in the Tasman and Coral Seas. Aust J Mar Freshw Res 16:151–162

Jitts HR (1969) Seasonal variations in the Indian Ocean along

110° E. IV. Primary production. Aust J Mar Freshw Res 20:65–75

Jones DA, Trewin BC (2000) On the relationships between the El Niño–Southern Oscillation and Australian land surface temperature. Int J Climatol 20:697–719

Kalnay E, Kanamitsu M, Kistler R, Collins W and others (1996) The NCEP/NCAR 40-year reanalysis project. Bull Am Meteorol Soc 77:437–471

Kamykowski D, Zentara SJ, Morrison JM, Switzer AC (2002) Dynamic global patterns of nitrate, phosphate, silicate, and iron availability and phytoplankton community composition from remote sensing data. Global Biogeochem Cycles 16, 1077, doi:10.1029/2001GB001640

Koslow JA, Pesant S, Feng M, Pearce AF and others (2008) The effect of the Leeuwin Current on phytoplankton biomass and production off Southwestern Australia. J Geophys Res 113, C07050, doi:10.1029/2007JC004102

Lee RS, Ajani P, Krogh M, Pritchard TR (2001) Resolving climatic variance in the context of retrospective phytoplankton pattern investigations off the east coast of Australia. J Coast Res 34:74–86

Lee RS, Pritchard TR, Ajani PA, Black KP (2007) The influence of the East Australia Current eddy field on phytoplankton dynamics in the coastal zone. J Coast Res 50:576–584

Levitus S, Antonov J, Boyer TT (2005) Warming of the world ocean, 1955–2003. Geophys Res Lett 32, L02604, doi: 10.1029/2004GL021592

Levitus S, Burgett R, Boyer T (1994) World ocean atlas 1994, Vol 3. Salinity. NOAA, Washington, DC

Longhurst A (1995) Seasonal cycles of pelagic production and consumption. Prog Oceanogr 36:77–167

Longhurst A (1998) Ecological geography of the sea. Academic Press, San Diego, CA

Lund JWG, Kipling C, Le Cren ED (1958) The inverted microscope method of estimating algal numbers and the statistical analysis of estimations by counting. Hydrobiologia 11: 143–170

Major GA, Dal Pont G, Klye JL, Newell BS (1972) Laboratory techniques in marine chemistry: a manual. CSIRO Division of Fisheries and Oceanography Report No. 51, CSIRO, Melbourne

Makridakis S, Wheelwright SC, Hyndman RJ (1998) Forecasting: methods and applications, 3rd edn. John Wiley, New York

McLean-Padman J, Padman L (1991) Summer upwelling on the Sydney inner continental shelf: the relative role of local wind forcing and mesoscale eddy encroachment. Cont Shelf Res 11:321–345

McQuatters-Gollop A, Raitsos DE, Edwards M, Attrill MJ (2007) Spatial patterns of diatom and dinoflagellate seasonal cycles in the NE Atlantic Ocean. Mar Ecol Prog Ser 339:301–306

Murphy J, Riley JP (1962) A modified single-solution for the determination of phosphate in natural waters. Anal Chim Acta 27:31–36

Oke PR, Brassington GB, Griffin DA, Schiller A (2008) The Bluelink ocean data assimilation system (BODAS). Ocean Model 21:46–70

Oke PR, Middleton JH (2001) Nutrient enrichment off Port Stephens: the role of the East Australian Current. Cont Shelf Res 21:587–606

Paasche E (1973) Silicon and the ecology of marine plankton diatoms. II. Silicate-uptake kinetics in five diatom species. Mar Biol 19:262–269

Parsons TR, Maita Y, Lalli CM (1984) A manual of chemical and biological methods for seawater analysis. Pergamon Press, Oxford

Pearce AF, Lynch MJ, Hanson C (2006) The Hillarys Transect (1): seasonal and cross-shelf variability of physical and chemical water properties off Perth, Western Australia, 1996–98. Cont Shelf Res 26:1689–1729

Pearce AF, Pattiaratchi CB (1999) The Capes Current: a summer countercurrent flowing past Cape Leeuwin and Cape Naturaliste, Western Australia. Cont Shelf Res 19:401–420

Platt T, Denman KL (1975) Spectral analysis in ecology. Annu Rev Ecol Syst 6:189–210

Plattner GK, Joos F, Stocker TF (2002) Revision of the global carbon budget due to changing air–sea oxygen fluxes. Global Biogeochem Cycles 16, 1096, doi:10.1029/2001GB001746

Pritchard TR, Lee RS, Ajani PA, Rendell PS, Black K, Koop K (2003) Phytoplankton responses to nutrient sources in coastal waters off southeastern Australia. Aquat Ecosyst Health Manag 6:105–117

Redfield AC (1958) The biological control of chemical factors in the environment. Am Sci 46:205–221

Richardson AJ, Poloczanska E (2008) Ocean science: underresourced, under threat. Science 320:1294–1295

Richardson AJ, Schoeman DS (2004) Climate impact on plankton ecosystems in the Northeast Atlantic. Science 305:1609–1612

Ridgway KR (2007) Long-term trend and decadal variability of the southward penetration of the East Australian Current. Geophys Res Lett 34, L13613, doi:10.1029/2007GL030393

Ridgway KR, Dunn JR (2003) Mesoscale structure of the mean East Australian Current System and its relationship with topography. Prog Oceanogr 56:189–222

Ridgway KR, Godfrey JS (1997) Seasonal cycle of the East Australian Current. J Geophys Res 102:22921–22936

Rochford DJ (1975) Nutrient enrichment of east Australian coastal waters. II. Laurieton upwelling. Aust J Mar Freshw Res 26:233–243

Rosenzweig C, Casassa G, Karoly DJ, Imeson A and others (2007) Assessment of observed changes and responses in natural and managed systems. In: Parry ML, Canziani OF, Palutikof JP, van der Linden PJ (eds) Climate change 2007: impacts, adaptation and vulnerability. Contribution of Working Group II to the Fourth Assessment Report of the Intergovernmental Panel on Climate Change. Cambridge University Press, Cambridge, p 79–131

Roughan M, Middleton JH (2002) A comparison of observed upwelling mechanisms off the east coast of Australia. Cont Shelf Res 22:2551–2572

Rudjakov JA (1997) Quantifying seasonal phytoplankton oscillations in the global offshore ocean. Mar Ecol Prog Ser 146:225–230

Sarmiento JL, Slater R, Barber R, Bopp L and others (2004) Response of ocean ecosystems to climate warming. Global Biogeochem Cycles 18, GB3003, doi:10.1029/2003GB002134

Scavia D, Field JC, Boesch DF, Buddemeier RW and others (2002) Climate change impacts on U.S. coastal and marine ecosystems. Estuaries 25:149–164

Schiller A, Oke PR, Brassington G, Entel M, Fielder R, Griffin DA, Mainsbridge JV (2008) Eddy-resolving ocean circulation in the Asian-Australian region inferred from an ocean reanalysis effort. Prog Oceanogr 76:334–365

Schmitt RW, Bogden PS, Dorman CE (1989) Evaporation minus precipitation and density fluxes for the North Atlantic. J Phys Oceanogr 19:1208–1221

Sverdrup HU (1953) On conditions for the vernal blooming of phytoplankton. J Cons Cons Int Explor Mer 18:287–295

Thompson PA (1998) Spatial and temporal patterns of factors

limiting phytoplankton in a salt wedge estuary, the Swan River, Western Australia. Estuaries 21:801–817

Thompson PA, Bonham PI, Swadling KM (2008) Phytoplankton blooms in the Huon Estuary, Tasmania: top-down or bottom-up control? J Plankton Res 30:735–753

Thompson PA, Pesant S, Waite AM (2007) Contrasting the vertical differences in the phytoplankton biology of a warm core versus cold core eddy in the south-eastern Indian Ocean. Deep-Sea Res II 54:1003–1028

Timbal B (2004) Southwest Australia past and future rainfall trends. Clim Res 26:233–249

Timbal B, Arblaster J, Power S (2006) Attribution of the late-twentieth-century rainfall decline in Southwest Australia. J Clim 19:2046–2062

Tranter DJ, Carpenter DJ, Leech GS (1986) Coastal enrichment effect of the East Australian Current eddy field. Deep-Sea Res A 33:1705–1728

Wiltshire KH, Malzahn AM, Wirtz K, Greve W and others (2008) Resilience of North Sea phytoplankton spring bloom dynamics: an analysis of long-term data at Helgoland Roads. Limnol Oceanogr 53:1294–1302

Wright SW, Jeffrey SW, Mantoura RFC, Llewellyn CA, Bjørnland T, Repeta D, Welschmeyer N (1991) Improved HPLC method for the analysis of chlorophylls and carotenoids from marine phytoplankton. Mar Ecol Prog Ser 77:183–196

Wood ED, Armstrong FAJ, Richards FA (1967) Determination of nitrate in sea water by cadmium-copper reduction to nitrite. J Mar Biol Assoc UK 47:23–31

Wood EJF (1954) Dinoflagellates in the Australian region. Aust J Mar Freshw Res 5:171–351

Wood EJF (1964) Studies in microbial ecology of the Australasian region. Nova Hedwigia 8:453–568

Appendix 1. Derivation of Θ_{100}, the fraction of East Australian Current (EAC) water

The origin of the water that resides on the continental shelf at Port Hacking at a particular time is a function of the past strength and direction of currents. In order to avoid specifying a particular time period (as the appropriate time span will vary with current strength), a simple numerical model has been constructed using velocity fields from a data-assimilating hydrodynamic model BlueLink Reanalysis (BRAN) that has been verified against observations (Oke et al. 2008, Schiller et al. 2008). The Θ_{100} parameter is derived from a simple model that considers a box with an area 1 m wide by 1 m deep in a cross-shelf plane, and 100 km in the alongshelf direction, which is flushed by water from either the north (EAC water) or the south (Tasman Sea water). The rate of flushing depends on the magnitude of the depth-averaged alongshore current. The time derivative of the fraction of EAC water, Θ_{100}, is given by $\Theta_{100}' = (v^- - |v|\Theta_{100})/L$, where v is the depth-averaged alongshore current (negative = southwards) at Port Hacking (obtained from BRAN), v^- is the depth-averaged alongshore current in the roughly southward direction (i.e. if $v < 0$, $v^- = -v$, else $v^- = 0$) and L is the alongshore length of the box. As an example, a constant current of 1 m s^{-1} into the 100 km long box will be diluted to 1/e of the original contents in 100 km × 1000 m km^{-1}/86400 s d^{-1} = 1.16 d. During the 10 yr analysis period, the flushing time of the box was generally 10 to 20 d. Over time, Θ_{100} varied between 0 and 1 but the mean monthly average values over 10 yr varied between a minimum in June of 0.6 and a maximum in August of 0.85

Editorial responsibility: Katherine Richardson, Copenhagen, Denmark

Submitted: April 29, 2009; Accepted: September 3, 2009
Proofs received from author(s): November 2, 2009